



HAL
open science

Dual role of alkoxyamine-functionalized lamellar materials in the synthesis of hybrid polymers

Prabhakar Sunchu, Eric Besson, Trang N.T. Phan, Stéphane Gastaldi

► To cite this version:

Prabhakar Sunchu, Eric Besson, Trang N.T. Phan, Stéphane Gastaldi. Dual role of alkoxyamine-functionalized lamellar materials in the synthesis of hybrid polymers. *European Polymer Journal*, 2024, 211, pp.112956. 10.1016/j.eurpolymj.2024.112956 . hal-04547715

HAL Id: hal-04547715

<https://cnrs.hal.science/hal-04547715v1>

Submitted on 16 Apr 2024

HAL is a multi-disciplinary open access archive for the deposit and dissemination of scientific research documents, whether they are published or not. The documents may come from teaching and research institutions in France or abroad, or from public or private research centers.

L'archive ouverte pluridisciplinaire **HAL**, est destinée au dépôt et à la diffusion de documents scientifiques de niveau recherche, publiés ou non, émanant des établissements d'enseignement et de recherche français ou étrangers, des laboratoires publics ou privés.

Dual Role of Alkoxyamine-Functionalized Lamellar Materials in the Synthesis of Hybrid Polymers

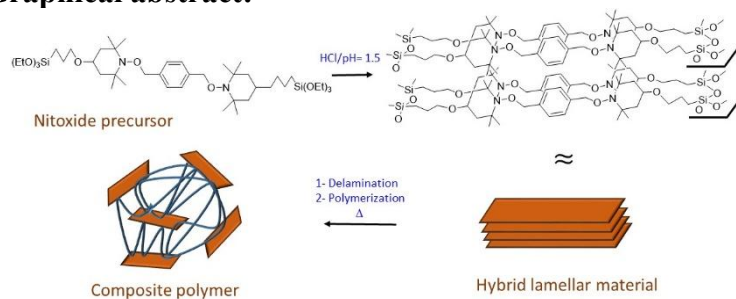
Prabhakar Sunchu,^a Eric Besson,^a Trang N. T. Phan^a and Stéphane Gastaldi^{a*}

^aAix Marseille Univ, CNRS, ICR, Marseille, France

Corresponding Author

eric.besson@univ-amu.fr; stephane.gastaldi@univ-amu.fr; trang.phan@univ-amu.fr.

Graphical abstract:



Abstract: Alkoxyamine-functionalized polysilsesquioxane lamellar materials were used as fillers and radical polymerization initiator in the synthesis of nanocomposites. This work is divided into three parts: (i) the synthesis and the characterization of functionalized-lamellae, (ii) the study of their delamination and (iii) the polymerization leading to the nanocomposites. The presence of covalently bonded siloxane filler reinforced the polystyrene. In addition, the EPR analysis showed that alkoxyamine groups were still present on the nanocomposite and could be homolyzed under thermal condition to enable further potential functionalisations.

Keywords: Nanofiller; Polysilsesquioxanes; Exfoliation; Nitroxide mediated polymerization

Introduction

Development of new nanocomposite materials, in which at least one of the phases has one-dimension less than 100 nm, is of topical interest in modern technology to enable

advances in fields such as health, transport, energy or nanotechnologies.¹ The characteristics of nanocomposite materials depend on the properties of the constituent phases, their relative amounts, the form of the dispersed phase and their synergistic interactions. The dispersed phases, commonly called nanofillers (NFs), can be particulate (carbon black, silica nanoparticle, polyhedral oligomeric silsesquioxane (POSS)), fibrous (nanofibers or carbon nanotubes) or layered nanomaterial (graphite, layered silicate and minerals).² Thus, the volume fraction, i.e. large interaction surface, and spatial arrangement of the NFs, the quality of adhesion between the phases and the dispersion, have a significant effect on the resulting properties of the nanocomposite. These hybrid materials can be classified into two classes depending on the nature of the interface between the phases. In the first class, Class I, the organic and inorganic interact via weak interactions (Van der Waals, hydrogen....) whereas in the second class, Class II, inorganic and organic compounds are linked by covalent or ionic bonds.³

Even though Class I materials are easy to prepare by mixing the two components in solid form or in solution using a solvent common to both, their main drawbacks lie in the fact that they do not exhibit a perfect homogeneity at the molecular or nanometric level. Furthermore, the weakness of the interactions between the NF and the matrix excludes specific applications because the NF could be released from the composites.⁴

When an organic phase and an inorganic phase are covalently bonded while controlling their dispersion, resulting CLASS II materials can exhibit original properties. For example, they can be used as sensor, catalyst or even as optical materials, avoiding release of the different components.⁵

One of the main difficulties of the composites development lies in the level of dispersion of NFs in the matrix. Indeed, a homogeneous dispersion of the fillers in the

host matrix is not always guaranteed because of the low compatibility between the constituents. In the case of nanoclay-based nanocomposites, three degrees of classification are generally adopted: tactoids, intercalated or exfoliated.⁶

Different strategies can be used to process complex multifunctional nanocomposites: (i) from molecular precursors or (ii) from well-defined nano-objects. The first route is based on the bottom-up approach and involves the synthesis of materials through soft chemistry processes (sol-gel process, metal-organic frameworks (MOF) synthesis, hydrothermal synthesis) from *well-designed precursors*. The second way, probably the most used, involves the use of pre-formed nano-objects (nanoparticles, nano sheets, polymers ...) as starting NF.⁷

Among the various fillers used in nano-composite materials, polysilsesquioxanes (PSQs) have been the subject of particular attention. PSQs are of general formula $[R-SiO_{1.5}]$ and can be prepared as random, ladder, lamellar, cage or partial cage structures.^{8,9,10} They exhibit thermal, mechanical, and chemical stability due to the presence of Si-O-Si bonds framework compared to C-C bonds. Moreover, thanks to the presence of different organic groups R, it is possible to modulate the nature of the organic functional groups of the material, which makes them compatible with great number of organic polymers. Nevertheless, attention has essentially been focused on silsesquioxanes with a cage structure, referred as POSS for polyhedral oligomeric silsesquioxane.¹¹ Ladder-like materials have also been incorporated into polymers but the literature is less rich and in the case of lamellar materials it is very sparse.¹²

Recently, we have shown¹³ that polysilsesquioxane-based lamellar materials, functionalized with diazene radical precursors, can play a double role in the preparation of nanocomposite materials: first, as filler homogeneously dispersed in the monomer after delamination, second as radical initiator in photopolymerization. Thanks to their ability to generate free radicals

upon light exposure, their behaviour as photoinitiator of polymerization of acrylate monomers at 365 nm was investigated and demonstrated. These experiments highlight that exfoliated nanosheets were suitable to initiate photopolymerization and enable nanocomposites with fillers covalently linked to the polymer.

In light of these results and in the aim to extend this approach to other polymerization systems we have investigated the synthesis of polystyrene (PS) nanocomposites obtained by nitroxide mediated polymerization (NMP) of styrene initiated by functionalized lamellar polysilsesquioxane. In this paper, we described the sol-gel synthesis and self-assembly of a bis-alkoxyamine functionalized lamellar polysilsesquioxane and the effect of the nature of the sol-gel catalyst on the lamellar polysilsesquioxane and their delamination. These fillers were then used as NMP initiator for the preparation of PS nanocomposite and the impact of the presence of NF on the viscoelastic properties of the resulting material was studied. This double bottom-up approach should lead to materials in which the components are homogeneously distributed and covalently bonded, which should have an impact onto the physico-chemical properties.

Experimental section

Materials. 2,2,6,6-Tetramethylpiperidine 1-oxyl, 2,2,6,6-Tetramethyl-1-piperidinyloxy (TEMPO), 4-hydroxy-TEMPO, 4,4'-bipyridine, allyl bromide, triethoxysilane and styrene were purchased from Sigma-Aldrich and used as received. Tetraethylorthosilicate (Sigma-Aldrich) was distilled before used. Other solvents and reactants were purchased from commercial suppliers and used without further purification. The bis-alkoxyamine **1** was prepared according to a literature procedure (Scheme 1).¹⁴

Lamellar polysilsesquioxanes synthesis (Scheme 2)

LAM-A: A suspension of **1** (1.0 g) in 20 mL of water at pH = 1.5 (acidified with hydrochloric acid) was stirred 10 min at room temperature then put in an oven at 90°C without stirring for 7 days. After cooling to room temperature, the mixture was filtrated through a sintered funnel (no. 4) and the solid residue was washed with water (2 times), followed by ethanol (3 times), acetone (2 times) then finally with diethyl ether (2 times). After 24 h under vacuum at 50 °C, a solid was recovered (200 mg). ¹³C CPMAS NMR (101.6 MHz) δ (ppm): 137.1 (*C_{ar}*), 128.1 (*CH_{Ar}*), 79.3 (*C*), 70.6 (OCH₂, OCH), 60.5 (OCH₂Ph, OCH₂), 58.4 (SiOCH₂), 45.7 (CH₂), 33.9 (CH₃), 24.0 (CH₂), 21.7 (CH₃), 18.9 (SiOCH₂CH₃), 9.7 (*SiCH₂*). ²⁹Si CPMAS NMR (79.5 MHz) δ (ppm): -45.4 (T¹), -58.1 (T²), -65.7 (T³). WAXS (nm⁻¹): broad signals : 2.25, 12.84.

LAM-B: To a stirred solution of **1** (1.0 g) in THF (2.4 mL) at room temperature was added a solution of THF/H₂O/HCl (THF (8.7 mL)/distilled H₂O (0.76 mL)/ HCl (37%) (23 μL)). The mixture was stirred 10 min then the stirring was stopped and the reaction let at room temperature for 6 days. Then the temperature was raised to 50 °C for 5 days until gelation. After cooling to room temperature, the mixture was filtrated through a sintered funnel (no. 4) and the solid residue was washed with water (2 times), followed by ethanol (3 times), acetone (2 times) then finally with diethyl ether (2 times). After 24 h under vacuum at 50 °C, a solid was recovered (830 mg). ¹³C CPMAS NMR (101.6 MHz) δ(ppm): 137.2 (*C_{ar}*), 129.7 (*CH_{Ar}*), 79.6 (*C*), 70.6 (OCH₂, OCH), 60.5 (OCH₂Ph, OCH₂), 45.0 (CH₂), 33.9 (CH₃), 22.1 (CH₂, CH₃), 9.8 (*SiCH₂*). ²⁹Si CPMAS NMR (79.5 MHz) δ(ppm): -57.4 (T²), -65.2 (T³). WAXS (nm⁻¹): broad signals : 3.15, 11.66.

LAM-C: Under Argon, to a stirred solution of **1** (1.0 g) in THF (1.5 mL) at room temperature was added a solution of THF/H₂O/TBAF (THF (19.55 mL)/distilled H₂O (1.84 mL)/ TBAF (1M in THF) (0.35 mL)). The mixture was stirred 10 min then the stirring was stopped and

the reaction let at room temperature for 2 h. Then the temperature was raised to 30 °C for 6 days until gelation of the solution, then the temperature was raised a second time to 50°C for 1 day. After cooling to room temperature, the mixture was filtrated through a sintered funnel (no. 4) and the solid residue was washed with water (2 times), followed by ethanol (3 times), acetone (2 times) then finally with diethyl ether (2 times). After 24 h under vacuum at 50 °C, a solid was recovered (1.08 g). ¹³C CPMAS NMR (101.6 MHz) δ(ppm): 137.1 (*C_{ar}*), 128.3 (*CH_{Ar}*), 79.2 (*C*), 70.5 (*OCH₂*, *OCH*), 60.2 (*OCH₂Ph*, *OCH₂*), 45.6 (*CH₂*), 33.7 (*CH₃*), 21.5 (*CH₂*, *CH₃*), 9.5 (*SiCH₂*). ²⁹Si CPMAS NMR (79.5 MHz) δ(ppm): -66.5 (*T³*). WAXS (nm⁻¹): broad signals : 2.77, 5.00, 11.21.

General procedure of polymerization. Lamellar material and DMF were added in a 2-neck round bottle flask fitted with reflux condenser. The mixture was degassed by bubbling of Argon for 10 minutes and stirred at room temperature for 2h to get the delamination. After this period, degassed styrene was added under argon and allowed to stir for additional 14h at RT except the experiment of entry 3 (Table 1), the additional stirring was only 3h. The system was immersed in an oil bath at 130 °C to allow the polymerization to occur. The polymerization was stopped after several days by rapid cooling and exposure of the polymerization solution to air. The resulting product was then dissolved in tetrahydrofuran and precipitated in methanol. The final polymer was filtered and dried under vacuum to a constant weight. Different polymerizations were carried out by varying experimental conditions. Experimental data of these polymerizations are summarized in Table 1. The mol number of initiators (*n_{initiator}*) in lamellar materials was calculated as $n_{initiator} = m_{lamellar\ mater.} / M_{bialkoxyamine}$ where $M_{bialkoxyamine} = 634 \text{ g mol}^{-1}$ corresponding to $\text{Si}_2\text{O}_3\text{C}_{32}\text{H}_{54}\text{N}_2\text{O}_4$ monomer units that compose the lamellar structure. The target molar mass (*M_n*) of polystyrene in experiments using lamellar materials as initiator (Table 1, entries 2 – 7) is

given for information to comparing with the one using free alkoxyamine as initiator (Table 1, entry 1) but in no case does it mean the true value of the target M_n of polystyrene.

Table 1. Experimental polymerization conditions

	Initiator	Delamination time (h)	m _{initiator} (mg)	n _{initiator} (mmol) ^a	m _{styrene} g (mmol)	m _{DMF} (mL)	Target M _n (mol g ⁻¹) ^b	Polym. time (days)	Styrene conversion (%)
1	3	0	45	0.100	2.00 (19.2)	0	20000	2	97%
2	LAM-C	16h	50	0.079	0.46 (4.37)	0	5822	5	67%
3	LAM-C	5h	50	0.079	0.46 (4.37)	0	5822	6	99%
4	LAM-C	16h	100	0.157	0.46 (4.37)	0	2929	6	95%
5	LAM-C	16h	50	0.079	0.46 (4.37)	0.1	5822	8	95%
6	LAM-B	16h	50	0.079	0.46 (4.37)	0.1	5822	8	100%
7	LAM-C	16h	200	0.315	1.82 (17.5)	0	5777	8	98%

^a n_{initiator} is the mol number of initiator calculated by formula: $n_{\text{initiator}} = m_{\text{lamellar mater.}} / M_{\text{bialkoxyamine}}$ where $M_{\text{bialkoxyamine}} = 634 \text{ g mol}^{-1}$ excepting entry 1 where $M_{\text{bialkoxyamine}}$ was replaced by the molar mass of bis-alkoxyamine 3.

^b Target M_n was calculated by formula $M_{n \text{ target}} = m_{\text{styrene}} / n_{\text{initiator}}$

General procedure for degrafting of PS chains from silica lamellae hybrid materials. In

a general experiment, 100 mg of dried hybrid material are weighted into a polypropylene tube. Then 5 mL of THF and 0.1 mL of HF (46%wt in H₂O) are added (Caution: HF is extremely corrosive). The reaction is left under stirring for 48h at 40°C. The mixture is neutralized with an excess of CaCO₃ for 30 min. The solution is filtered and concentrated under reduced pressure. 5 mL of an aqueous solution of NaOH (10% wt) and 5 mL of DCM are added to the tube. After stirring, organic phase is recovered, dried over MgSO₄, filtered, and precipitated in methanol to recover the degrafted PS polymer chains.

Characterization techniques.

Thermogravimetric (TGA) measurements were carried out on a 5 mg sample with a PerkinElmer 8000 instrument at a scan rate of 10 °C.min⁻¹ from 40 to 800°C under dynamic air atmosphere at a flow rate of 20 mL.min⁻¹.

Differential Scanning Calorimetry (DSC) experiments were carried out on a TA Instruments DSC Q20. The measurements were performed by heating around 10 mg of samples from 50°C or 80°C to 130°C for hybrid material and commercial PS respectively. The heating rate was 10°C min⁻¹. The glass transition temperature (T_g) was determined on the transition of the

second heating cycle of the thermograms and was chosen at the 50% change of the heat capacity that is close to the point of inflection.

Wide angle X-ray scattering (WAXS) experiments were performed on SAXSess-MC2 (Anton-Paar, GmbH, Austria) with a sealed copper tube as X-ray source (wavelength is 0.15417 nm (Cu K- α)) equipped with a Kratky block-collimation system and using an image plate (IP 200 \times 60 mm, pixel resolution 50 \times 50 μ m) as detector. The system operates in line collimation, which allows achieving higher scattering intensities and image. Plate are read with the Cyclone (Perkin Elmer) and Optiquant software system. An exposure time of 30 minutes was long enough to provide a good signal-to-noise ratio (scattering angle range $0.1 < q < 28 \text{ nm}^{-1}$). SAXSquant was used as data analysis software.

All solid-state Cross Polarization Magic Angle Spinning (CPMAS) NMR spectra were obtained on a Bruker Avance-400 MHz NMR spectrometer operating at a ^{13}C and ^{29}Si resonance frequency of 101.6 MHz and 79.5 MHz, respectively. ^{13}C and ^{29}Si CPMAS experiments were performed with a commercial Bruker Double-bearing probe. About 100 mg of samples were placed in zirconium dioxide rotors of 4-mm outer diameter and spun at a Magic Angle Spinning rate of 10 kHz. The CP technique¹⁵ was applied with a ramped ^1H -pulse starting at 100% power and decreasing until 50% during the contact time in order to circumvent Hartmann-Hahn mismatches.^{16,17} The contact times were 2 ms for ^{13}C CPMAS and 5 ms for ^{29}Si CPMAS. To improve the resolution, a dipolar decoupling GT8 pulse sequence¹⁸ was applied during the acquisition time. To obtain a good signal-to-noise ratio, 6144 scans were accumulated using a delay of 2 s in ^{13}C CPMAS experiment, and 4096 scans with a delay of 5 s in ^{29}Si CPMAS experiment. The ^{13}C and ^{29}Si chemical shifts were referenced to tetramethylsilane.

Viscoelastic properties of polystyrene composite were studied using an Anton Paar Rheometer MCR 302 equipped with 25 mm diameter aluminium parallel disks. The polymer

was pressed to a gap width of 0.9 mm. The complex shear modulus, $G^* = G' + iG''$, was then measured as a function of frequency by dynamically shearing the polymer at a fixed strain of 1% over the frequency range 0.01 to 600 rad s^{-1} at 160°C. All measurements were performed in a dry air atmosphere.

Size exclusion chromatography (SEC) analysis were performed on an EcoSEC apparatus from PSS, equipped with a dual flow cell refractive index detector. Eluent was THF at a flow rate of 0.3 $\text{mL}\cdot\text{min}^{-1}$ for the sample pump and 0.15 $\text{mL}\cdot\text{min}^{-1}$ for the reference pump. The stationary phase was a combination of one PL Resipore (50x4.6) mm guard column and two PL Resipore (250x4.6) mm columns thermostated at 40°C. Samples were prepared by dissolving 10 mg of sample in 2 mL of THF containing 0.25 vol.% of toluene, as a flowmarker. The soluble fraction of sample was filtered through 0.45 μm PTFE filters. Injection volume was 20 μL . Polystyrene equivalent number-average and weight-average molar masses (M_n and M_w respectively) and dispersities D were calculated by means of PS calibration curve using PS-M Easivial standards (Agilent, USA).

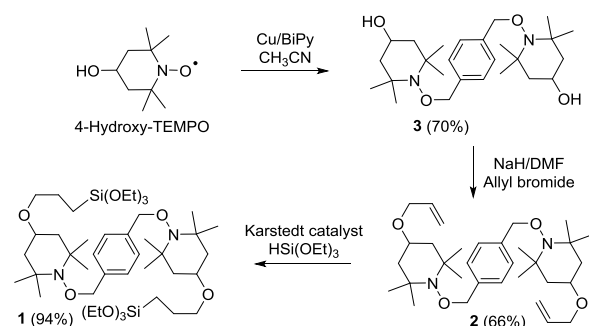
Dynamic light scattering (DLS) measurements were performed on a Malvern Nanosizer ZS- apparatus equipped with a He–Ne laser operating at a wavelength of 633 nm. The temperature was controlled at 25 °C. The method of the cumulants was used to analyze DLS results.

Preparation of samples for DLS analysis. Under light protection, a suspension of lamellar material (**LAM-A**, **LAM-B** or **LAM-C**) (10 mg, 0.5 wt%) was stirred in 2 mL of one of the solvent listed in Table 2 for 24h. A solution was prepared for each analysis. Then two measurements were performed: (i) at 0s, 1 ml was directly taken from the stirred solution and poured into the DLS analysis cell and the analysis was run or (ii) the stirring was stopped and

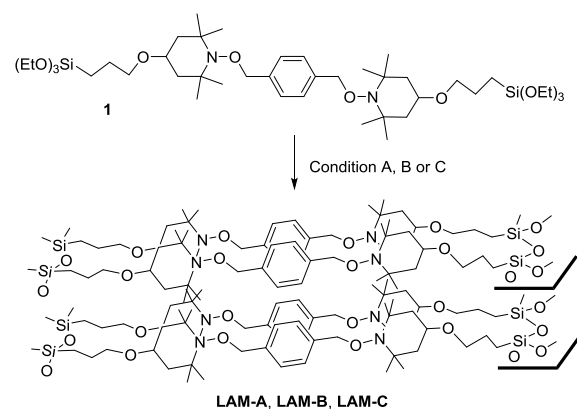
after 60s, 1 ml was taken from the solution and poured into the DLS analysis cell and the analysis was run.

Results and Discussion

Synthesis of lamellar materials. Three functionalized polysilsesquioxane-based lamellar materials were prepared according to the synthesis process presented in Scheme 2. The bis-silylated alkoxyamine **1**^{14,19} was the basic unit for the preparation of lamellar NF. Its symmetrical structure was designed to facilitate the characterization of the lamellar material. Indeed, a non-symmetrical alkoxyamine would lead to a lamellar structure incorporating head-to-head and head-to tail coupling during its formation, which would have complicated its characterization. Initiators **1** was readily synthesized from the corresponding bis-benzylbromide in three steps (Scheme 1): (1) introduction of 4-hydroxy-TEMPO on the benzyl skeleton, (2) allylation and (3) introduction of trialkoxysilane groups through hydrosilylation.



Scheme 1. Synthesis of bis-alkoxyamine **1**.



A: HCl/H₂O, 90°C. B: THF/HCl/H₂O (1.5 eq/Si), RT. C: THF/TBAF/H₂O (1.5 eq/Si).

Scheme 2. Synthesis of lamellar polysilsesquioxanes **LAM-A**, **LAM-B** and **LAM-C** from **1**.

Lamellar materials **LAM-A**, **LAM-B** and **LAM-C** were prepared from precursor **1** using different conditions thanks to the sol-gel process (Scheme 2). It must be stressed that due to the thermal fragility of the benzyl alkoxyamine unit it is not possible to use a protocol involving a temperature higher than 50°C, therefore soft procedures were selected. The experimental conditions have a direct impact on the processes governing the structuring of the material. Firstly in an aqueous medium at pH 1.5, the pre-organisation of organic precursors results from hydrophobic interactions emphasized by the solvent (**LAM-A**).^{20,21} By contrast, in an organic solvent (THF) and under acidic (HCl (**LAM-B**)) or nucleophilic catalysis like tetra-*n*-butylammonium fluoride (TBAF) (**LAM-C**), the pre-organisation relies only on interactions between the organic precursors without an additional external stress.²⁰ The resulting lamellar materials were characterized by classical methods such as ¹³C and ²⁹Si solid state NMR (SS NMR) and XRD. ¹³C SS NMR analysis confirmed the stability of the organic precursor under the sol-gel process conditions, all the characteristic signals were recorded for the three materials (Figures S1 - S3). For example, in the case of **LAM-C**, the spectrum showed the presence of the aromatic ring (137.1 (C) and 128.3 ppm (CH)), the benzylic position (79.2 ppm (CH₂)), the carbons in alpha position of the oxygen atom (70.5 ppm (CH and CH₂)) and the carbon in alpha position of the silicon atom (9.54 ppm (CH₂)). ²⁹Si SS NMR clearly emphasized a difference between the ratio of *T*¹ (RSi(OH)₂OSi), *T*² (RSi(OH)(OSi)₂) and *T*³ (RSi(OSi)₃) siloxane structures (Figure 1). Concerning **LAM-A**, in addition of the presence of trialkoxysilane (-45.4 ppm) a mixture of *T*¹, *T*² (signal at around -58 ppm), and *T*³ (-65 ppm) siloxane structures were clearly identified indicating an incomplete polycondensation. For **LAM-B** and **LAM-C**, only two signals at -57 ppm and -66 ppm attributed to *T*² and *T*³ signals were registered but their relative intensities showed a

more efficient polycondensation for **LAM-C** since only a small shoulder was observed for T^2 structure.

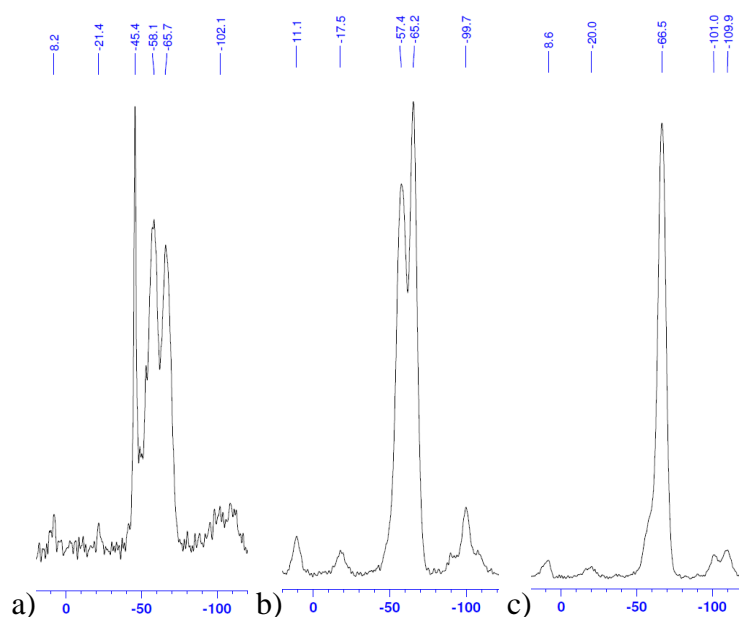


Figure 1. ^{29}Si NMR spectra of **LAM-A** (a), **LAM-B** (b) and **LAM-C** (c).

The WAXS scattering patterns displaying the scattering intensity $I(q)$ as a function of the scattering vector q of lamellae sample at room temperature and are shown in Figure 2. The WAXS analyses allowed to deepen the characterization of these materials and to determine which synthesis protocol was the best adapted to our organic precursor to obtain the best structuring of the lamellar material. As expected, no characteristic peak was observed for **LAM-A** indicating the absence of a lamellar structure due to an incomplete polycondensation of silica precursor. For the materials prepared in THF, **LAM-B** and **LAM-C**, the diffractograms displayed 1st order peaks (3.15 and 2.77 nm^{-1}) compatible with the length of the organic precursor estimated by molecular modelling at 29.2 \AA . Additional peaks (2nd and 4th order, 5.0 and 11.2 nm^{-1} respectively) were detected for **LAM-C** indicating a better structuring for this material. The characterization of these materials clearly showed that the use of an organic solvent favoured a better structuring of lamellae in the case of our radical precursor.

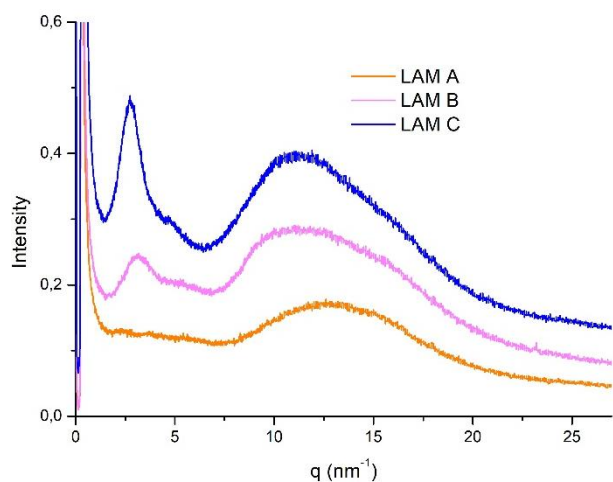


Figure 2. WAXS analyses for **LAM-A**, **LAM-B** and **LAM-C**

Delamination study of lamellae materials. The second phase of this study aimed to use lamellar materials as both radical initiator and filler in the synthesis of hybrid materials. But first, it was necessary to find conditions under which these materials could delaminate in order to have a homogeneous dispersion of lamellae in the organic medium and thus a better access to initiator moieties. Since **LAM-A** material is less-structured than the **LAM-B** and **LAM-C** materials, the delamination study was only carried out on **LAM-B** and **LAM-C**. Dynamic light scattering (DLS) was selected to monitor their delamination process in different solvents with representative polarities (apolar, basic polar, protic polar)²² (Table 2). Ethylbenzene (EtPh) was selected as mimic of styrene, monomer of subsequent polymerization.

The DLS analysis was performed after stirring the lamellar materials for 24h in the solvents listed in table 2. The comparison of the object size in different solvents clearly showed that a delamination was observed with solvents whose polarity is higher than that of dichloromethane. In these solvents, the size of the objects ranged from 35 to 9 nm whereas in less polar solvent like EtPh, the object size was considerably higher than 1000 nm. 60 s after stopping the magnetic stirring, an aggregation of the objects was recorded for all samples

indicating that agitation should be maintained for any application involving these nanofillers.

Longer agitation time about 48 h and 72 h did not allow better results.

Table 2. DLS analysis of **LAM-B** and **LAM-C** after 24h.

Solvent (E_T) ^a	LAM-B		LAM-C	
	Object size (nm) at different time after stopping the magnetic stirring			
	0s	60s	0s	60s
EtPh (E_T 34.1)	1110	1433	420	631
Styrene (E_T 34.8)	966	1220	885	1445
CH ₂ Cl ₂ (E_T 40.7)	35	53	18	42
DMA (E_T 42.9)	17	58	23	61
DMF (E_T 43.2)	9	62	12	43
<i>n</i> BuOH (E_T 49.7)	12	45	5	16
EtOH (E_T 51.9)	11	50	9	67
MeOH (E_T 55.4)	14	39	28	40
DMF:Styrene (1:3; vol/vol)			498 ^b	1236 ^b
DMF:Styrene (1:1; vol/vol)			74 ^b	630 ^b
			35 ^c	68 ^c
DMF:EtPh (1:1; vol/vol)			113 ^d	231 ^d
			29 ^c	58 ^c

^a Polarity parameter. ^b Styrene as reference. ^c DMF as reference. ^d Ethylbenzene as reference.

In order to use these lamellae as both nanofiller and radical initiator of styrene polymerization, it was important that the delamination occurred in the presence of styrene. In the least polar solvents, i.e. EtPh and styrene, and under agitation **LAM-C** seems more delaminated than the **LAM-B**. For this reason, the study of the influence of a co-solvent was only performed on **LAM-C**. DMF was chosen as co-solvent because of its ability to delaminate and its compatibility with a radical polymerization process. 33 and 100% of DMF were added to styrene but only the second ratio enabled the delamination to occur almost as efficiently as in the DMF. Comparable results were obtained with a mixture of DMF/EtPh (50/50, v/v) indicating that no side reaction took place with the styrene throughout the process.

To ensure that alkoxyamine molecules in lamellae materials will be available and accessible to the polymerization of styrene, the homolysis of alkoxyamine in **LAM-C** was investigated by EPR spectroscopy. For that, a suspension of **LAM-C** in tert-butylbenzene in a EPR quartz tube was heated under air at 130°C, the formation of the corresponding nitroxide by

homolysis of alkoxyamine was readily observed (Figure 3). The quantification, performed with a standard solution of TEMPO, showed that 40% of the alkoxyamine moieties were homolyzed although lamellae material was not delaminated before carrying EPR analysis. This result indicated that the rigid structure of lamellae did not hinder the homolysis of alkoxyamine. It must be underlined that the homolysis also occurred at solid state (see SI, Figure S4-S5).

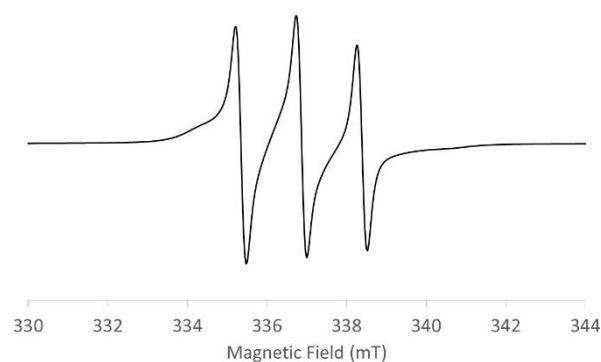


Figure 3. EPR spectrum of **LAM-C** in *tert*-butylbenzene recorded at 25°C after heating at 130°C

NMP of styrene using lamellae materials. The NMP of styrene was first performed in the presence of bis-alkoxyamine **3** using as model initiator. Polymerization was carried out in bulk at 130°C for 48h. However, the styrene conversion was almost complete after 21h (see SI, Figure S10). For these two polymerizations, the experimental molecular weights of the derived polystyrene (PS) were very different to the theoretical values, calculated from the feed ratio of styrene to bis-alkoxyamine, and the dispersities of obtained PS were higher than the acceptable dispersity of 1.5 for a controlled radical polymerization process (Table 3). TEMPO-mediated polymerization of styrene derivatives was largely studied in the literature.^{23,24} Hawker obtained a better control of styrene polymerization than us in similar conditions by using a monoadduct prepared by heating a mixture of benzoyl peroxide, TEMPO and an excess of styrene at 80°C.²⁵ The unwell-control of styrene polymerization in

the present study can be explained by the low dissociation rate of the bis-alkoxyamine **3**. Indeed, **3** is a primary alkoxyamine while that used by Hawker was a secondary alkoxyamine. In consequence, the resulting transient radicals of the dissociation of **3** are less efficient in the initiation reaction with styrene.

The use of **LAM-B** and **LAM-C** as NMP initiator was performed in different polymerizations of styrene. The polymerization was carried out either in bulk or in solution using DMF as solvent. Although the optimal condition for an efficient delamination of lamellar materials in the mixture of styrene/DMF was the 1:1 ratio (vol/vol), as indicated in the previous section and Table 2. However, preliminary polymerization experiments carried out in these conditions using lamellar materials, as initiator required extremely long reaction times, so we carried out styrene polymerization either in pure styrene or in a styrene/DMF ratio of 5:1 (vol/vol). The reaction conditions are detailed in Table 1. The results showed that the kinetic of styrene polymerization using **LAM-C** as initiator was extremely low compared to that using bis-alkoxyamine **3**. The dispersity of resulting PS was also high (Table 3). The high dispersity values suggest a contribution of (thermal) self-initiation process of styrene at these temperatures. Typically, this process leads to polymer chains with high M_n in the range of 200000 – 300000 g.mol⁻¹.²⁶ However, M_n values of our synthesized polystyrene (fraction of soluble PS in hybrid material) were not exceeded of 50000 g.mol⁻¹ (Table 3, columns 5). Of course, this does not totally exclude the presence of PS chains formed by (thermal) self-initiation process but their detection in the SEC chromatograms is not evident, hence they may be considered negligible.

We note that whatever the experimental conditions used (initiator nature, polymerization condition and styrene/initiator ratio), the experimental M_n (determined by SEC) are all higher than those of theoretical M_n and decreased when the amount of initiator increased (entries 2 and 4, Table 1). Keeping in mind that the sample solution injected on SEC measurements was

the soluble fraction of the hybrid material dissolved in THF, the solvent used for SEC analysis. These results were expected and can be explained by the fact that not all initiator sites were accessible to styrene. So, the efficient initiator sites were fewer than expected, contributing to an increase in the M_n of PS chains. Furthermore, the PS chains analyzed by SEC are probably the PS free chains liberated from lamellae or the small fraction of soluble silica lamellae/PS hybrid materials. In the latter case, PS chains are linked to lamellae material, and therefore the experimental M_n determined by SEC express the length not of one PS chain but probably several chains grafted to silica lamellae.

To check our first hypothesis that the sample analyzed by SEC contained only PS free chains, the PS chains were degrafted from silica lamellae by using HF solution and then analyzed by SEC. The M_n of degrafted chains and their dispersities are given in Table 3. It was accepted and also demonstrated that in Surface-Initiated Controlled Radical Polymerization (SI-CRP), the M_n and the dispersity of grafted chains are almost equal to the values of the free polymers.²⁷ For experiments carried out in bulk (Table 3, entries 2, 4 and 7), the M_n and dispersity values of degrafted chains and those of hybrid materials are very similar. In contrast, the M_n and the dispersity values of degrafted chains and hybrid materials are quite different in experiments performed in the presence of DMF (Table 3, entries 5 and 6). This difference could be attributed to possible transfer reactions with the DMF solvent. Since the M_n and the dispersity of degrafted PS and hybrid PS are similar, we can consider that the soluble fraction of hybrid material dissolved in THF contained only free PS chains detached from silica lamellae.

The results also showed that the experimental conditions affected both molar mass and dispersity of the final material. For example, a short delamination time led to an increase of polymer dispersity (entries 2 and 3, Table 1 and Table 3) as well as the use of DMF as polymerization solvent (entries 4 and 5, Table 3). The increase of dispersity in experiment 2

compared to experiment 3 is attributed to an unwell-delamination of LAM-based alkoxyamine making initiator less accessible to monomer. In a similar polymerization condition, the use of **LAM-B** as initiator led to polystyrene material having M_n five times lower than that obtained with **LAM-C** as initiator (entries 5 and 6, Table 3). Although the delamination of **LAM-B** was less efficient than that of **LAM-C** (see previous section, Table 2), the structure of **LAM-B**, less organized and unwell-defined compared of **LAM-C** (see WAXS characterization), could explain the higher accessibility of initiator sites to monomer in **LAM-B** than in **LAM-C** material and therefore a lower M_n in **LAM-B**. On the other hand, for a similar process with larger quantity of reactants and using the same **LAM-C** as initiator (Table 1 and Table 3, entries 2 and 7), an increase of styrene conversion did not lead to PS material with higher molar masse as often observed in NMP process. Indeed, the molar masse of the sample obtained in experiment 7 is lower than the one obtained in experiment 2 (Table 3) although the targeted M_n is similar in both experiments and conversion of styrene was higher in experiment 7. In such system, the control of polymerization at high monomer conversion became less efficient because the low diffusion of TEMPO specie as agent control causing in one hand by an increasing of medium viscosity and on other hand by the anchoring of TEMPO to silica lamellar restrict the mobility of the latter. The resulting hybrid materials were also analyzed by TGA (see SI, Figure S8). The wt% of residual silica at 700°C is reported in Table 3. As expected, all samples contain the same wt% of silica since the initial ratio of lamellar material to styrene was identical with the exception of experiment 4 where the amount of lamellar material was doubled, leading to a final hybrid material with higher wt% of silica. The experimental wt% of residual silica is slightly higher than the expected value (around 1.8 wt%). These results can be explained by the fact that TGA measurements were carried out under air atmosphere, so the transformation of silica under $\text{SiO}_{1.5}$ form in lamellae to SiO_2 form after TGA analysis led to a gain in mass of silica.

Table 3. Characteristics of the hybrid materials synthesized from the lamellar materials reported in Table 1.

Entry	Initiator nature	Polym. condition	M_n (th) ^a mol g ⁻¹	M_n , SEC ^b mol g ⁻¹	\bar{D}	M_n , degrafted ^c mol g ⁻¹	\bar{D} , degrafted	% wt of silica ^d
1	3	bulk	19400	14800	1.8	-	-	0
2	LAM-C	bulk	3901	49600	1.8	48200	1.9	2.7
3	LAM-C ^e	bulk	5764	46900	2.4	- ^f	-	- ^f
4	LAM-C	bulk	2783	19600	1.5	18600	1.6	4.7
5	LAM-C	DMF	5531	41100	2.2	31800	3.1	2.8
6	LAM-B	DMF	5822	7900	2,3	11100	1.7	2.6
7	LAM-C	bulk	5661	37400	1.9	38100	2.0	2.9

^a The theoretical M_n was calculated by applying the formula M_n (th) = target M_n * styrene conversion.

^b M_n of polystyrene determined by SEC from the soluble fraction of hybrid sample.

^c M_n of polystyrene chains degrafted from hybrid materials and determined by SEC

^d wt% of residual silica in the composites determined by TGA at 700 °C.

^e The delamination time of LAM-B and LAM-C at room temperature in the polymerization mixture was fixed for 16h (overnight) before starting the polymerization at 130°C excepting experiment of entry 4 where the delamination time was 5h.

^f The quantity of hybrid materials was insufficient to perform the degrafting experiments.

To study the impact of delamination time on the structure of the resulting hybrid polystyrene, WAXS analyses were carried out on the polystyrene made after 5 and 16 h of delamination (entries 2 and 3, Table 3) and compared with those of LAM-C (Figure 4). Two main informations were provided by these analyses. Firstly, the characteristic peak correlated with the bis-alkoxyamine length (2.77 nm^{-1}) disappears as delamination time increases possibly indicating better homolysis on unstacked lamellae. Secondly, considering LAM-C before delamination (blue line, Figure 4), the diffractogram displayed a broad peak between 7.00 and 20.00 nm^{-1} . The latter encompassed two characteristic signals, the interlamellae and the interchain distances. After 16 h of stirring in styrene, followed by polymerization (green line, Figure 4), this peak became sharper, which could be explained by the disappearance of the interlamellar part, confirming delamination. The remaining peak at 13.6 nm^{-1} , corresponding to a characteristic interchain distance of 0.45 nm in a polysilsesquioxane, showed that the filler was incorporated into polystyrene with its features.

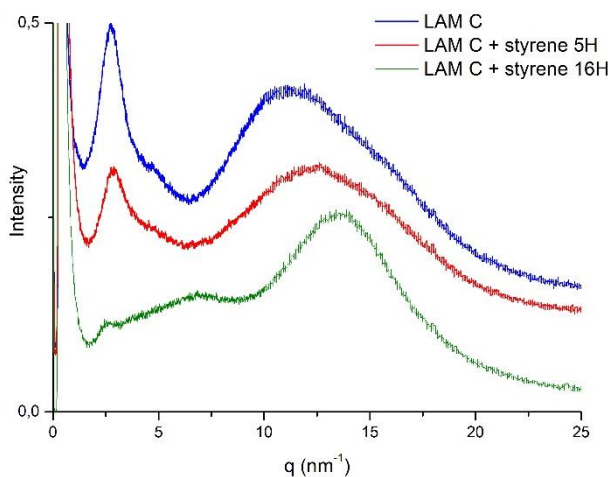


Figure 4. Comparison of WAXS analyses of **LAM-C** and nanocomposites prepared after 5h or 16h of delamination.

The living character of the resulting nanocomposite was assessed by heating a sample (entry 2, Table 3) in *tert*-butylbenzene at 130°C in a EPR spectrometer probe (Figure 5A). A strong signal of TEMPO was quickly recorded demonstrating the material's ability to generate alkyl radicals and thus initiate new polymerizations. The same behavior occurred at solid state (see SI, Figure S6-S7). The quantity of TEMPO radicals was estimated by EPR and achieved a yield of 77%, compared with 40% for **LAM-C** in a similar analysis time. The comparison of the homolysis kinetics of the nanocomposite and **LAM-C** revealed a very different profile (Figure 5B). In the case of the nanocomposite, the growth was rapid before reaching a plateau (about 800s) whereas, with **LAM-C**, the growth was slow and the plateau was only reached after 3 days. These two behaviors highlighted different surroundings. Indeed, the low mobility of the alkoxyamine in the lamellae structure of **LAM-C**, due to the aggregation of lamellae, and hence their poor delamination state together with the reversibility of the homolysis considerably slowed down this process. In the contrary, the lamellae were separated in the resulting nanocomposite, due to the repulsion interactions of polystyrene chains, increasing the homolysis rates.

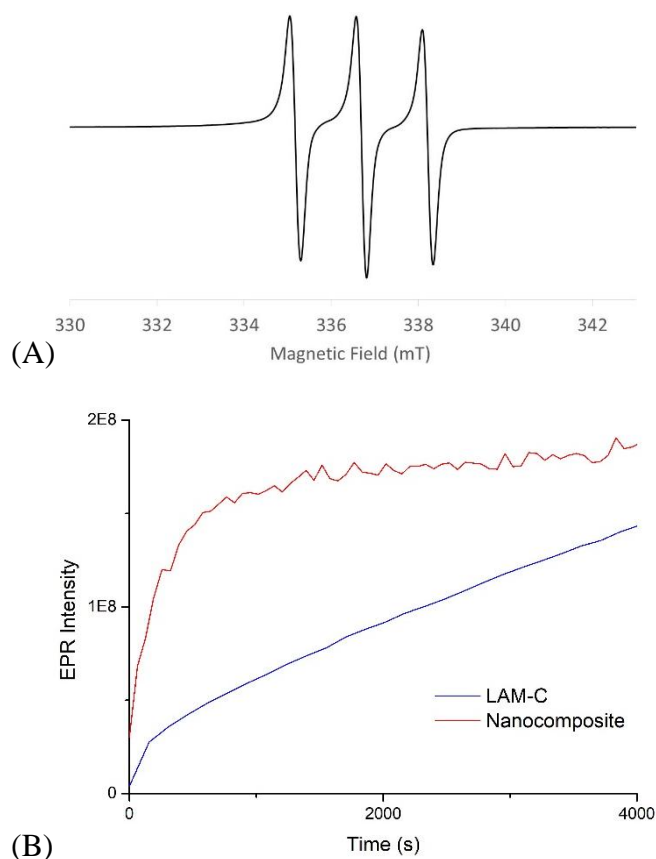


Figure 5. (A) EPR spectrum of nanocomposite prepared from **LAM-C** in tert-butylbenzene recorded at 25°C after heating at 130°C. (B) Homolysis kinetics of **LAM-C** and the nanocomposite.

Viscoelastic properties of PS/silica lamellar composite, sample of experiment 7 (Table 3, entry 7) and pure PS are presented in Figure 6. It is obviously apparent from Figure 6 that PS/silica lamellar composite show an improvement in viscoelastic properties even at low silica lamellar weigh fraction of around 3%. It must be noted an increase of both elastic (G') and loss (G'') modulus six times higher than those of pure PS of similar M_n especially at low frequencies. At high oscillation frequencies, the effect of silica lamellar is relatively weak, however transition from solid-like ($G' > G''$) to liquid-like ($G' < G''$) viscoelastic behaviour occurred at lower frequencies in PS/silica lamellar composite compared to pure PS. This improvement was not due to the big difference of glass transition temperature (T_g) between commercial PS and synthesized PS/silica lamellar composite since their T_g values are 100°C

and 104°C respectively (Figure S9). This result illustrates a good reinforcement of PS by silica lamellar at only a small weigh fraction of the latter.

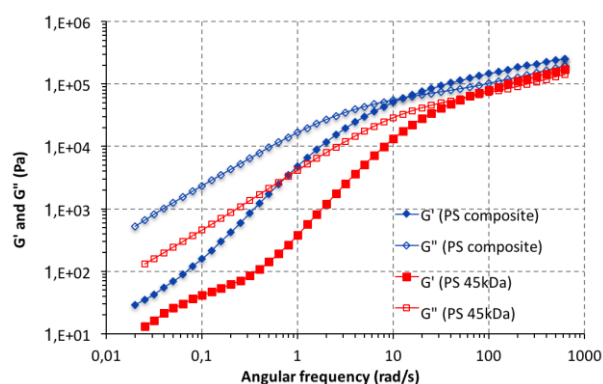


Figure 6. Viscoelastic properties of grafted PS/silica lamellar composite compared to a commercial PS of 45 kg.mol⁻¹. Measurements were performed at 160°C with a strain amplitude of 1%.

Conclusion

Alkoxyamine-functionalized lamellar hybrid materials were synthesized to prepare nanocomposite. This strategy was based on the structural control of the filler to obtain the lamellae morphology. Three conditions of the sol-gel process were evaluated for their preparation, the nucleophilic catalysis with fluoride led to lamellae with a well-defined structure. To optimize the filler distribution in the final composite, the delamination conditions of the lamellae were investigated in a wide range of solvents. DMF was then used as solvent for the styrene polymerization with the lamellae as radical initiator. These materials played a dual role both as filler and initiator of polymerization. This synthetic approach led to composites where all components were covalently linked together. Moreover, this double bottom-up approach avoids the filler dispersion problem encountered in the preparation of composite from pre-formed polymer. The presence of polysilsesquioxane in the composites had an impact on their viscoelastic properties demonstrating the reinforcement of the polystyrene by the lamellae.

CRedit authorship contribution statement

Prabhakar Sunchu: Investigation. **Eric Besson:** Supervision, Writing – original draft. **Trang N. T. Phan:** Supervision, Writing – original draft. **Stéphane Gastaldi:** Supervision, Writing – original draft.

Declaration of Competing Interest

The authors declare that they have no known competing financial interests or personal relationships that could have appeared to influence the work reported in this paper.

Data availability

No data was used for the research described in the article.

Acknowledgement

This project received funding from the A*MIDEX project (ANR-11-IDEX-0001-02) funded by the “Investissements d’Avenir” French Government program and managed by the ANR.

Appendix A. Supplementary data

Supplementary data to this article can be found online at

References

-
- ¹ M. Faustini, L. Nicole, E. Ruiz-Hitzky, C. Sanchez, History of Organic–Inorganic Hybrid Materials: Prehistory, Art, Science, and Advanced Applications, *Adv. Funct. Mater.* 28 (2018) 1704158, <https://doi.org/10.1002/adfm.201704158>.
- ² S. K. Sahu, V. Boggarapu, P.S.R. Sreekanth, Improvements in the mechanical and thermal characteristics of polymer matrix composites reinforced with various nanofillers: A brief review, *Mater. Today-Proc* (2024) in Press , <https://doi.org/10.1016/j.matpr.2023.07.032>.
- ³ L. Nicole, L. Rozes, C. Sanchez, Integrative approaches to hybrid multifunctional materials : from multidisciplinary research to applied technologies, *Adv. Mater.* 22 (2010) 3208–3214, <https://doi.org/10.1002/adma.201000231>.

-
- ⁴ I. Tiwari, P.A. Mahanwar, Polyacrylate/silica hybrid materials: A step towards multifunctional properties, *J. Dispersion Sci. Technol.* 40(7) (2019) 925–957, <https://doi.org/10.1080/01932691.2018.1489276>
- ⁵ B. Popanda, J. Grolík, W. Gieszczyk, M. Sroda, Effect of the sol-gel condition on photostability and optical properties of alkoxy-substituted zinc phthalocyanine in the hybrid glass matrix, *Dyes Pigm.* 213 (2023) 111142, <https://doi.org/10.1016/j.dyepig.2023.111142>
- ⁶ C.I. Idumah, M.C. Obele, E.O. Ezeani, Understanding interfacial dispersions in ecobenign polymer nano-biocomposites, *Polym-Plast. Technol. Mater.* 60 (2021) 233–252, <https://doi.org/10.1080/25740881.2020.1811312>.
- ⁷ P. Gomez-Romero, A. Pokhriyal, D. Rueda-García, L. N. Bengoa, R. M. González-Gil, Hybrid Materials: A Metareview, *Chem. Mater.* 36 (2024) 8-27, <https://doi.org/10.1021/acs.chemmater.3c01878>.
- ⁸ C. Zhang, C. Ma, X. Yao, X. Yang, W. Zhang, G. Zhang, Transparent and flexible vesicles/lamellae mixed matrix organic-bridged polysilsesquioxane coatings as water vapor barrier, *Prog. Org. Coat.* 174 (2023) 107236, <https://doi.org/10.1016/j.porgcoat.2022.107236>.
- ⁹ **M. Gamal Mohamed**, S.-W. Kuo, Progress in the self-assembly of organic/inorganic polyhedral oligomeric silsesquioxane (POSS) hybrids, *Soft Matter*, 18 (2022) 5535–5561, <https://doi.org/10.1039/D2SM00635A>.
- ¹⁰ K. Kajihara, K. Kanamori, A. Shimojima, Current status of sol-gel processing of glasses, ceramics, and organic-inorganic hybrids: a brief review, *J. Ceram. Soc. Jpn.* 130, 8 (2022) 575–583, <https://doi.org/10.2109/jcersj2.22078>
- ¹¹ F. Dong, L. Lu, C.-S. Ha, Silsesquioxane-Containing Hybrid Nanomaterials: Fascinating Platforms for Advanced Applications, *Macromol. Chem. Phys.* 220 (2019) 1800324, <https://doi.org/10.1002/macp.201800324>.

-
- ¹² F.M. Fernandes, C. Sanchez, Integrative strategies to hybrid lamellar compounds : an integration challenge, *App. Clay Sci.* 100 (2014), 2–21, <https://doi.org/10.1016/j.clay.2014.05.013>.
- ¹³ C. Dol, F. Vibert, M.P. Bertrand, J. Lalevée, S. Gastaldi, E. Besson, Diazene-Functionalized Lamellar Materials as Nanobuilding Blocks: Application as Light Sensitive Fillers to Initiate Radical PhotoPolymerizations, *ACS Macro Lett.* 6 (2017) 117–120, <https://doi.org/10.1021/acsmacrolett.6b00949>.
- ¹⁴ E. Besson, F. Ziarelli, E. Bloch, G. Gerbaud, S. Queyroy, S. Viel, S. Gastaldi, Silica materials with wall-embedded nitroxides provide efficient polarization matrices for dynamic nuclear polarization NMR, *Chem. Commun.* 52 (2016) 5531–5533, <https://doi.org/10.1039/C6CC01809B>.
- ¹⁵ J. Schaefer, E.O. Stejskal, Carbon-13 nuclear magnetic resonance of polymers spinning at the magic angle, *J. Am. Chem. Soc.* 98 (1976) 1031–1032, <https://doi.org/10.1021/ja00420a036>.
- ¹⁶ O.B. Peersen, X. Wu, I. Kustanovich, S.O. Smith, Variable-Amplitude Cross-Polarization MAS NMR, *J. Magn. Reson.* 104 (1993) 334–339, <https://doi.org/10.1006/jmra.1993.1231>.
- ¹⁷ R.L. Cook, C.H. Langford, R. Yamdagni, C.M. Preston, A modified cross-polarization magic angle spinning ¹³C NMR procedure for the study of humic materials, *Anal. Chem.* 68 (1996) 3979–3986, <https://doi.org/10.1021/ac960403a>.
- ¹⁸ G. Gerbaud, F. Ziarelli, S. Caldarelli, Increasing the robustness of heteronuclear decoupling in magic-angle sample spinning solid-state NMR, *Chem. Phys. Lett.* 377 (2003) 1–5, [https://doi.org/10.1016/S0009-2614\(03\)01056-X](https://doi.org/10.1016/S0009-2614(03)01056-X).
- ¹⁹ P. Nabokoff, S. Gastaldi, E. Besson, Probing the efficiency of thermal and photochemical bond homolysis in functionalized nanostructured SBA-15 silicas, *Micropor. Mesopor. Mat.* 311 (2021) 110674, <https://doi.org/10.1016/j.micromeso.2020.110674>.

-
- ²⁰ A. Abraham Chemtob, L. Ni, C. Croutxé-Barghorn, B. Boury, Ordered Hybrids from Template-Free Organosilane Self-Assembly, *Chem. Eur. J.* 20 (2014) 1790–1806, <https://doi.org/10.1002/chem.201303070>.
- ²¹ K. Kajihara, K. Kanamori, A. Shimojima, Current status of sol-gel processing of glasses, ceramics, and organic-inorganic hybrids: a brief review, *J. Ceram. Soc. Jpn.* 130 (2022) 575–583, <https://doi.org/10.2109/jcersj2.22078>.
- ²² A. Wypych, G. Wypych, *Databook of Solvents*, ChemTec Publishing, Toronto, 2019.
- ²³ G. Moad, E. Rizzardo, Chapter 1 : The History of Nitroxide-mediated Polymerization , in *Nitroxide Mediated Polymerization: From Fundamentals to Applications in Materials Science*, Gimes, D., Eds; Royal Society of Chemistry, 2015, 1-44, <https://doi.org/10.1039/9781782622635-00001>.
- ²⁴ A. Roggi, E. Guazzelli, C. Resta, G. Agonigi, A. Filpi, E. Martinelli, Vinylbenzyl Chloride/Styrene-Grafted SBS Copolymers via TEMPO-Mediated Polymerization for the Fabrication of Anion Exchange Membranes for Water Electrolysis, *Polymers* 15 (2023), 1826; <https://doi.org/10.3390/polym15081826>.
- ²⁵ C.J. Hawker, Molecular weight control by a "living" free radical polymerization process, *J. Am. Chem. Soc.*, 116 (1994) 11185–11186, <https://doi.org/10.1021/ja00103a055>.
- ²⁶ A. Nabifar, N. T. McManus, E. Vivaldo-Lima, L. M. F. Lona, A. Penlidis, Thermal polymerization of styrene in the presence of TEMPO. *Chem. Eng. Sci.* 64 (2009), 304–312. <https://doi.org/10.1016/j.ces.2008.10.013>.
- ²⁷ M. Bonnevide, T. N.T. Phan, N. Malicki, S. K. Kumar, M. Couty, D. Gimes, J. Jestin, Synthesis of polyisoprene, polybutadiene and Styrene Butadiene Rubber grafted silica nanoparticles by nitroxide-mediated polymerization. *Polymer*, 190 (2020), 122190, <https://doi.org/10.1016/j.polymer.2020.122190>.